ORIGINAL ARTICLE

Assessment of performance of horizontal drains in an open pit mine in eastern Turkey

Cidem Argunhan-Atalay[1] · Hasan Yazicigil[1] · Mehmet Ekmekci[2]

Abstract
Prediction of spatial distribution of pore-water pressure and its control are the main issues in open pit mines, since excess pore-water pressure is one of the main causes of slope instability. Horizontal drains are commonly used to relieve the excess pore-water pressure as a method of slope stabilization. This paper presents the efficacy of horizontal drains along two cross-sections in an open pit mine located in Eastern Turkey by analyzing the re-distribution of pore-water pressure as a consequence of groundwater inflow rates before and after application of horizontal drains. SEEP/W software was used to simulate the flow in saturated and unsaturated zones along North–South and East–West cross-sections. The accuracy of the input data was verified by calibrating the models under steady-state condition against the field data obtained from vibrating wire pressure transducers installed at different depths and locations. This was followed by a transient analysis to confirm the storage parameters. The results of the transient simulation run showed that steady-state model results can be used as initial conditions for transient groundwater inflow predictions. Subsequently, expansion and deepening of the open pit for the year 2019 are modeled in stage-wise for both cross-sections to calculate the groundwater inflow rates into the mine. As a last step, horizontal drains are implemented to the models. The horizontal drains increased groundwater inflow rates by only 15 and 37% for the East–West and North–South cross-sections, respectively. Additionally, the water content was found to be almost close to fully saturation state in the wall rock behind the slope faces even after the use of drains. The findings of this study were verified at the site. The mining company has reported that attempts to drain the slope walls by horizontal drains have proved to be ineffective. In conclusion, it was demonstrated that prevention of seepage from surface channels by either diversion or lining was adopted as opposed to horizontal drill holes as the most effective means of controlling groundwater influence on slope stability.

Keywords SEEP/W · Slope stability · Pore water pressure distribution · Open pit mine

Introduction

Stability of cut slopes is always associated with safety and economics in opencast mines. Economics can be improved by steepening the slopes, but steep slopes have the tendency to fail especially because of excessive pore-water pressures (Singh et al. 2013). Hence, prediction of pore-water pressure distribution and groundwater inflow in open pit mines are important issues, because pore water is one of the main contributory factors in slope instability. Pore water has two significant effects. First, increase in pore-water pressure results in reduction in the shear strength of the slope forming material, eventually affecting the slope stability. The second is the seepage force associated with groundwater flow that triggers the slope instability (Mukhlisin and Abd-Aziz 2016). The role of pore-water pressure in open pit slopes has been recognized since early times and studied by different researchers (Harman et al. 2007; Ulusay et al. 2014; Solak et al. 2017).

Pore-water pressure can be modified by different means (Beale and Read 2013). Dissipation of pore-water pressure can be achieved under natural conditions by allowing seepage to the slope. If seepage under natural gradient does not provide sufficient dissipation of pore-water pressure, dewatering and/or depressurization methods should

✉ Hasan Yazicigil
hyazici@metu.edu.tr

[1] Geological Engineering Department, Middle East Technical University, 06800 Ankara, Turkey

[2] Hydrogeological Engineering Program, Hacettepe University, 06800 Ankara, Turkey

be applied for slope stability. Depressurization is generally applied as a method of slope stabilization when high pore-water pressure values exist in low permeable materials. Horizontal drains are commonly used to reduce pore-water pressure for depressurization purpose in open pits (Leech and McGann 2008; Harman et al. 2007). Horizontal drains are also commonly used in relieving the pore-water pressure in earth dam slopes and landslides (McNicholl et al. 1986; Resnick and Znidarcic 1990; Ghiassian and Ghareh 2008; Jia et al. 2009; Rahardjo et al. 2011; Cano and Tomás 2013; Moharrami et al. 2014).

The success of horizontal drains in dissipating pore-water pressures, however, depends largely on detailed hydrogeological characterization of the study area which will help to determine the feasibility of the drain system and its design characteristics (location, spacing, length, diameter, etc.). Martin et al. (1994) concluded that small number of drains installed at appropriate locations based on well-conceived conceptual model can increase the efficiency of drain systems. Hence, the value of horizontal drains depends on having reliable hydrogeological data and an accurate conceptual model. Reliable conceptualization is often followed by numerical model construction. With the advancement of modern computer technology, different numerical models are available to evaluate the role of pore-water pressure and the efficacy of horizontal drains for slope stability. Pit slope models are often based on 2D cross-section models which allow analysis of great level of complexity (Beale and Read 2013; Harman et al. 2007; Williams et al. 2007; Brehaut 2009; Douglas et al. 2009).

While the effectiveness of horizontal drains is substantially studied by many researchers (McNicholl et al. 1986; Resnick and Znidarcic 1990; Ghiassian and Ghareh 2008; Jia et al. 2009; Rahardjo et al. 2011) in landslide areas, the modeling studies that evaluate the effectiveness of horizontal drains in open pit mines are limited (Harman et al. 2007; Williams et al. 2007). Harman et al. 2007 used 2D numerical model to assess the effectiveness of the horizontal drains in hypothetical homogeneous and isotropic intact rock and in an intact rock with permeable fractures by analyzing the improvement in the factor of safety. They have concluded that while numerical modeling provides the best opportunity to assess the pore-water pressure distributions and the effectiveness of horizontal drains, the lack of importance that is generally given to adequate data gathering from field to be used as model input may end up a black-box approach with incorrect design result. Williams et al. (2007) used 2D numerical models to assist in designing a depressurisation program using horizontal drains and concluded that elevated pore-water pressures were not the primary cause of slope instability, but detailed geotechnical analyses of potential slope instability under 'saturated' conditions are required

to fully assess the effectiveness of the depressurisation program.

The cost associated with a slope depressurization program is always obvious and apparent, but the consequential benefits may not be. Therefore, in-depth hydrogeological field testing followed by numerical model simulations prior to the implementation of any slope depressurization program can allow mine management to develop trade-offs between the cost of implementing such a program against the benefits to be gained from the program. A large open pit mine located within a complex geological setting in eastern Turkey recently experienced installing pilot horizontal drain holes along some critical slopes with no in-depth hydrogeological data. The objectives of installing horizontal drains, however, were not fulfilled to the expectations. This study is conducted with the aim to determine if the installation of horizontal drains would be successful for slope depressurization after conducting in-depth hydrogeological field testing, conceptual and numerical model development, and performance evaluation. The scope of the study included hydrogeological characterization, conceptual model development, and numerical modeling of the whole cut slopes through the pit advancement for two cross-sections which are aligned in South–North and East–West directions with the help of SEEP/W software. The results obtained are expected to be of immediate value to the database of experience of the mining industry in understanding how various rock types with particular characteristics react under various drainage/depressurisation scenarios.

Site description

The Çöpler Gold Mine site is located in Eastern Turkey, about 7 km west of İliç town and 120 km west of the Erzincan city (Fig. 1). The mine is operated by Anagold Madencilik Sanayi and Ticaret AS in the form of a series of side-by-side open pits. The project includes three open pits that will merge into one super pit at the end of the mining activity. The study area is located within a kind of topographical depression captured by Çöpler stream, a small tributary of the Karasu River (Fig. 1). Karasu River bordering the study area from the north is the only perennial stream. Two streams are connected to the mine site: the Çöpler stream and the Sabırlı Stream. The Çöpler stream has almost completely been altered with mining operations.

Topographically, the mine area is located in an east–west oriented valley surrounded by high carbonate rock masses of the Munzur mountain range. The elevation of the valley ranges approximately between 1100 and 1300 m (asl), while the surrounding carbonate rocks reach an altitude of more than 2500 m in the south and a little less than 1500 m in the north sides of the mine site.
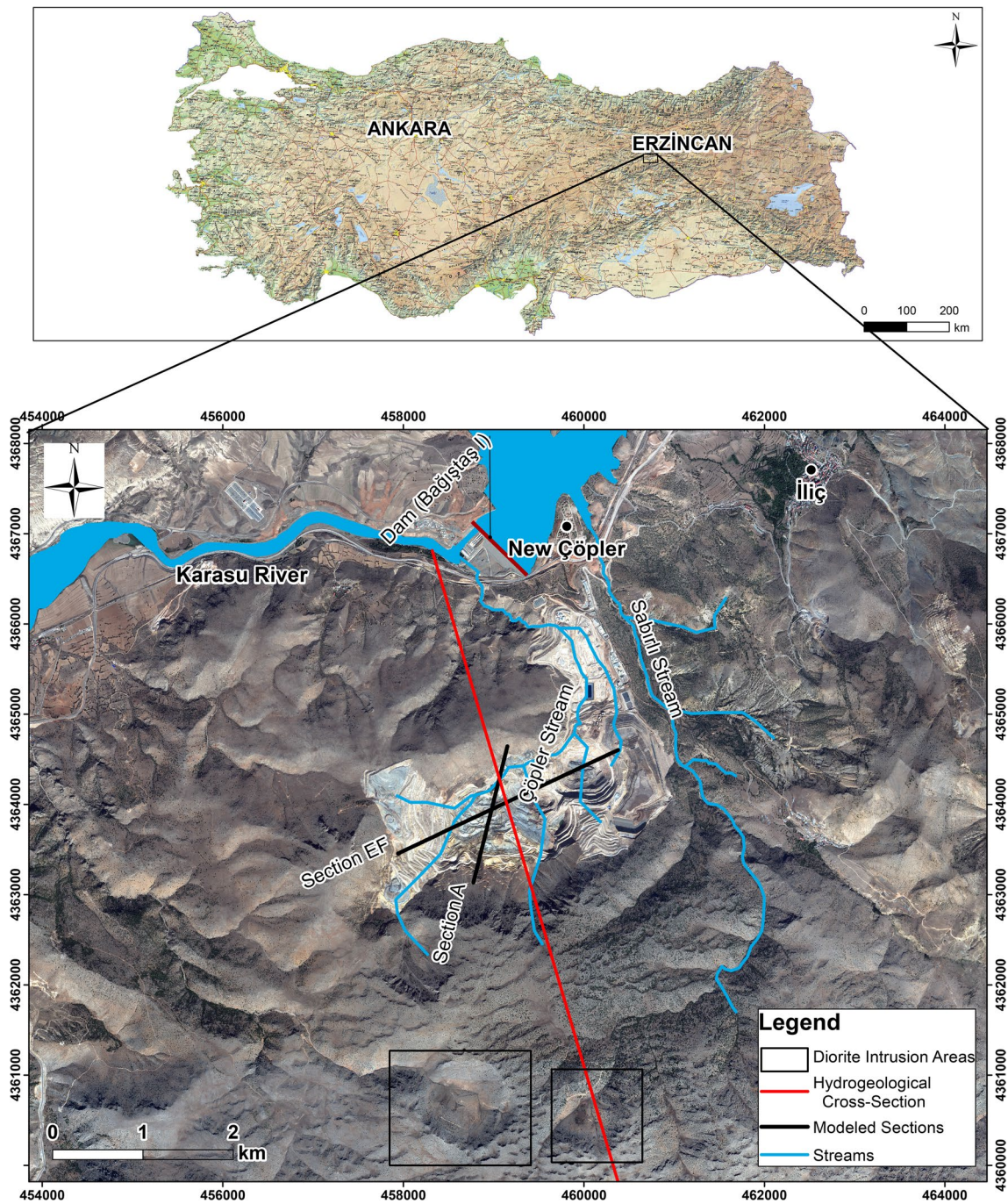
Fig. 1 Location of study area

The geological setting of the region including the project area has been studied at a 1/100,000 scale by Ozgul et al. (1981). Based on structure, stratigraphy, and metamorphism, Ozgul et al. (1981) have defined three "structural units" in the region, from bottom to top: Keban Unit, Munzur Dağı Unit (Munzur Limestone), and Ovacik Unit. These units are in tectonic contact with each other and covered by the post-tectonic deposits. Çöpler mine site is geologically located in

a metamorphic–magmatic complex surrounded by the Munzur Dağı Unit. The geological structure of the mine site is studied in detail for mine prospection. In Çöpler mine site, three main lithologies, namely the carbonate rocks (limestone and marble of the Munzur Formation), metasediments and diorite, and their alteration products, have been identified (Fig. 2). Munzur limestone has been metamorphosed to marble in the vicinity of the mine site due to magmatic
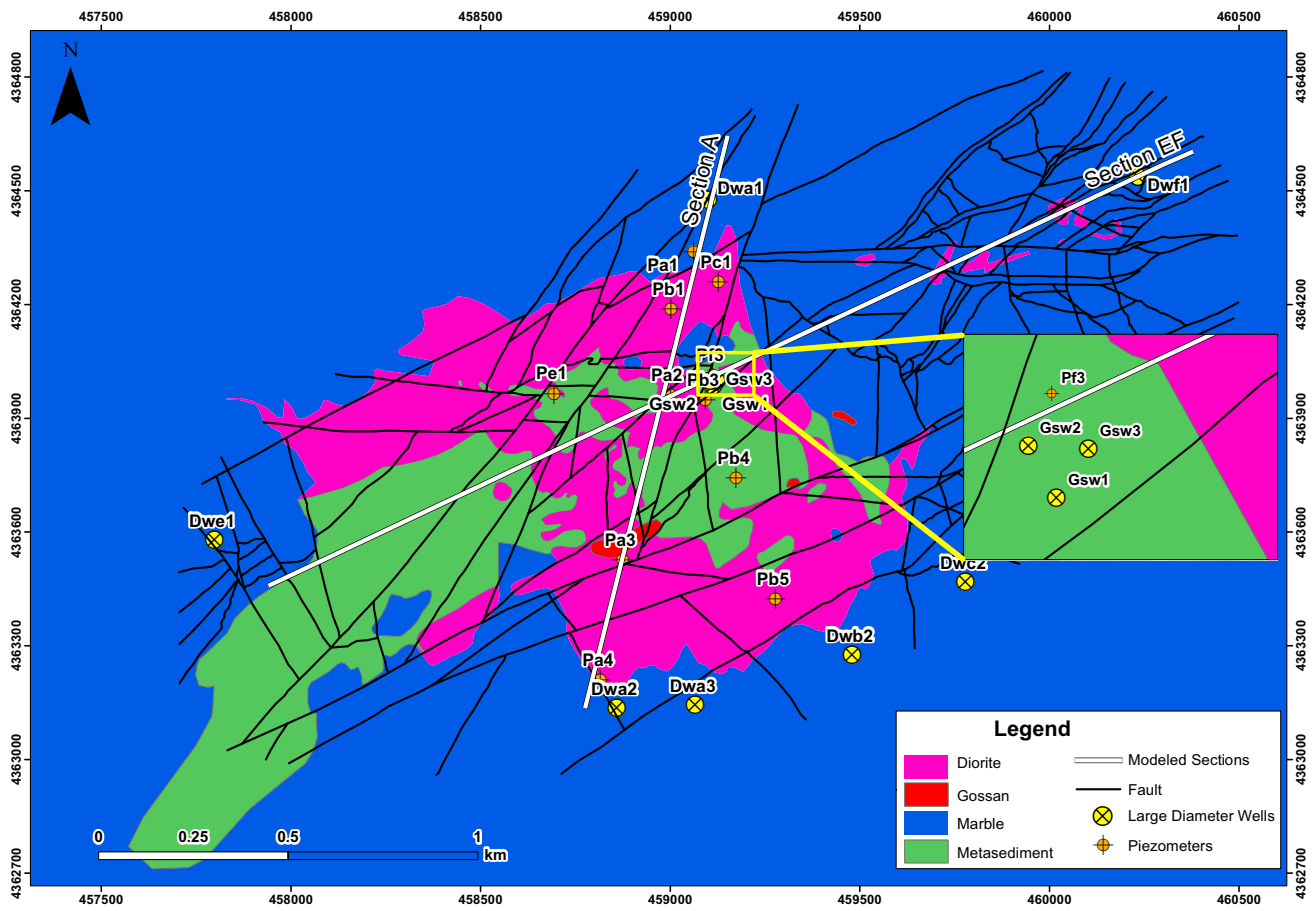
Fig. 2 Geology of the study area with the cross-sections studied (modified from Ekmekci et al 2018)

intrusions. Therefore, the carbonates in the mine area are named as marble in the remainder of the text. This unit displays various degrees of karst development. Bedding within the unit is indistinct to massive. Metasediments are defined as fine-grained argillite sequences consisting of interbedded siltstones, shale units, marls, and sandy siltstones. The thermal and hydrothermal impact to this unit from the magmatic intrusions resulted in the creation of the skarns and hornfels. Diorite intrusions are defined as beige and light brown, medium-to-coarse grained plutons. This formation has intruded into the pre-existing argillites and Munzur limestone. This includes fine- to medium-grained quartz, feldspar, biotite, and amphibole minerals (Alacer Gold 2016). The geology along the studied cross-sections was produced by Anagold geologists from the continuously updated database using the LeapFrog™ software.

The latest study on structural geology was conducted by Terrane Geoscience Inc. (2018), and nine different fault sets were defined based on similar orientation and common deformation history. The South Çöpler Fault Zone and series and sub-parallel faults represent the most recent faulting

activity that has divided the north and the south parts of the mine into two principal structural domains. Additionally, the North Çöpler Fault is modeled as steeply dipping, E–W-trending fault zone (Terrane Geoscience Inc. 2018).

The climate is typically continental with wet, cold winters and dry, hot summers. Meteorological records at Divriği station which is the most representative station for the study area are used for assessment of recharge. The long-term (1975–2016) average annual precipitation and air temperature recorded at Divriği meteorological station are 383 mm and 12.8 °C, respectively.

Hydrogeological characterization and conceptual model development

Hydrogeological properties of the lithological units were acquired by drilling large (17.5 inch) diameter wells and small (4.75 inch) diameter piezometer holes. There are totally 11 piezometer holes and 10 large-diameter wells drilled in the study area (Fig. 2) along the selected

cross-sections. The 11 small diameter drill holes were used to obtain data for geotechnical and hydrogeological characteristics of metasediments and diorite. To characterize groundwater condition and pore-water pressure distributions in these units, 33 vibrating wire piezometers were installed at various depths in the piezometer holes. In addition, 7 large-diameter wells were drilled to characterize the groundwater conditions and aquifer properties in the carbonate rocks surrounding the mine site and three wells in the metasediments within the active mine (Fig. 2).

To obtain permeability profile along the cross-sections, packer tests were conducted at 2-m test intervals in the PQ size (4.75 inch) piezometer holes. The test results were evaluated according to Roeper et al. (1992) to obtain representative permeability values (Ekmekci 2012; Vaskou et al. 2019). Packer test results revealed that the metasediments and the diorites have similar hydrogeological characteristics, and generally speaking, they can be regarded as one hydrostratigraphic unit. For example, geometric mean of the hydraulic conductivity of the diorites is 1.53×10^{-7} m/s, while geometric mean of the hydraulic conductivity for metasediments is 2.41×10^{-7} m/s. Additionally, porosity and water content values are similar for both units and they only differ if units are altered or massive. Hence, metasediments and diorite can be regarded as one hydrostratigraphic unit from the modeling point of view. However, faulting, folding, and different degrees of alteration have caused heterogeneity to some extent which required subdivision of this hydrostratigraphic unit into zones of different permeability. Delineation of distinct zones was based on packer test results, RQD, and textural properties. The arithmetic mean of hydraulic conductivity calculated from all data (totally 816 packer tests) is 1.0×10^{-6} m/s, while the geometric and harmonic means are 9.5×10^{-8} m/s and 2.1×10^{-9} m/s, respectively. The coefficient of variation is 359%, indicating a great heterogeneity. The hydraulic gradient at vibrating wire piezometers is mostly in a downward direction.

Pumping tests have been planned to obtain hydraulic characteristics of the carbonate rock aquifer and the metasediment–diorite unit. However, because the carbonate rock unit was dry in most of the large-diameter wells, pumping test could be conducted at only one well (Dwb-2) drilled in carbonate rock unit at southeastern part of the study area. In contrast to the high hydraulic conductivity values for carbonates in the northern part of the study area as reported by Golder (2013), a low value of 2.42×10^{-8} m/s has been obtained for the southern part of the domain. The hydraulic conductivity of the carbonates around mine site varies between 2.42×10^{-8} and 6.08×10^{-3} m/s, depending upon degree of karstification. The hydraulic conductivity values, ranging between 9.55×10^{-8} and 3.78×10^{-10} m/s, obtained from pumping tests conducted in wells drilled in metasediments and diorite units are even lower than those from

packer tests. This is not surprising because of the fact that packer tests represent more local characterization (Ekmekci et al. 2018). The pumping tests are representative for larger volumes.

The components of the water budget were calculated using the Monthly Thornthwaite Water Balance Model developed by McCabe and Markstrom (2007). Groundwater recharge was calculated on the basis of the water balance equation with an assumption of a soil storage capacity of 100 mm. The average annual groundwater recharge was found to be 33.6 mm for the mine site.

The Çöpler Groundwater System is composed of the Çöpler Stream basin, and includes carbonate rock masses consisting mainly of marbles surrounding the metasediment and diorite units in the center. The carbonate rock mass is karstified at least to a certain depth and, therefore, may form an aquifer. The metasediment and the diorite units hydrogeologically act as one hydrostratigraphic unit having lateral and vertical heterogeneity, and compared to the carbonate rocks, these units have low permeability. In previous studies, the vast carbonate rock mass extending in the south of the Çöpler stream basin is considered to supply groundwater inflow toward the Çöpler groundwater system. On the other hand, ore drillings in the south part of the area have revealed that a massive diorite intrusion may form a sort of barrier against groundwater flow from the south to north to the Çöpler groundwater system. A conceptualized hydrogeological cross-section illustrating the general flow conditions along the section shown in Fig. 1 which extends from south to north is given in Fig. 3.

According to the conceptual model illustrated in Fig. 3, the southern carbonate rock mass is divided into two parts: the larger part forming the main carbonate rock aquifer and the small part between the diorite intrusion and the metasediments cropping out at the mine site has a small area for recharge. In this part, one should not expect thick saturated zone. Apparently, the thin saturated zone is being discharged toward the west to contribute to the springs at the flood plain of the Karasu River and partly to the east to Sabırlı Stream. This conceptual model also explains the dryness of the wells drilled in carbonate rocks in this part of the area.

Based on the availability and recently obtained data, a hydrogeological conceptual model was constructed along Section A, as shown in Fig. 1 on which the numerical model is subsequently developed to assess the effectiveness of drains. The subsurface geology, in situ tests, and hydrochemical data were used in developing a representative conceptual model. The hydraulic characteristics of the metasediments and the diorite are very close. These two units are hydraulically interconnected and, therefore, can be assumed to form a single hydrostratigraphic unit having lateral and vertical heterogeneity for hydraulic conductivity distribution. The flow domain is bounded by permeable carbonate rocks.
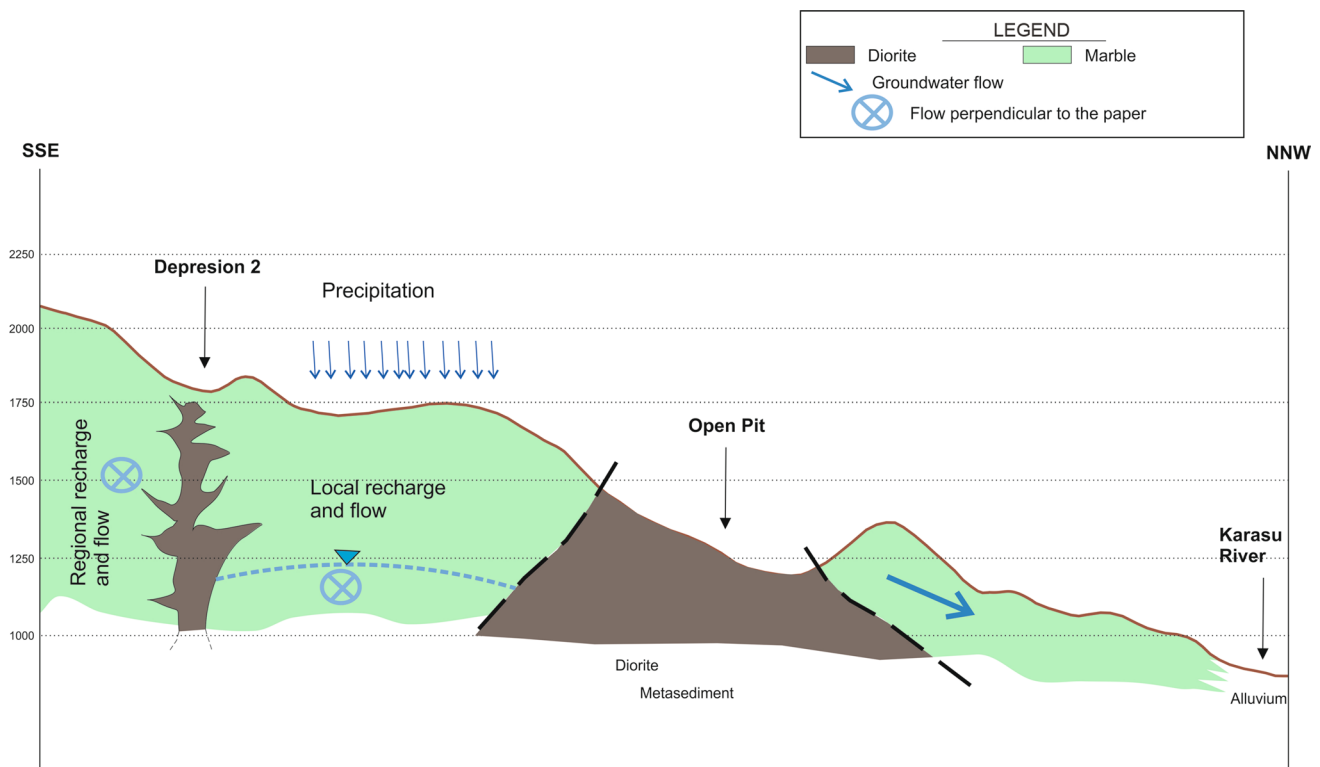
Fig. 3 Hydrogeological cross-section demonstrating the role of diorite intrusion in regional groundwater flow (Ekmekci et al. 2018)

Groundwater-level measurements reveal that the metasediments and the diorite are saturated almost all along the year with little fluctuations. The isotope data have confirmed the fact there is no groundwater flow to the flow domain from the surrounding carbonate rocks. Evaluation of stable isotopes has suggested that the origin of the pore water in metasediments and diorite units is mainly local precipitation (Ekmekci et al. 2018). In addition, the downward hydraulic gradient measured at the vibrating wire piezometers supports this finding.

The metasediments and the diorite have high total porosity (ranges between 22 and 6%) and low specific yield (ranges between 4 and 2%) which means that a great portion of the pore water is retained by the electrostatic forces in the material. It resists flowing because of the very low hydraulic conductivity. The medium is recharged by infiltration from direct precipitation and from surface runoff. The outflow must be occurring mainly by evapotranspiration. A generic conceptual model along Section A, which demonstrates the working hydrogeological system, is depicted in Fig. 4.

Numerical code

In this study, SEEP/W, a component of GeoStudio™ (Geo-Slope 2007), is employed to analyze pore-water pressure distribution under different topographic conditions in variably saturated porous media and to calculate the groundwater inflow to open pits. SEEP/W is a 2D finite-element model and can be used from simple, saturated steady problems to sophisticated, saturated/unsaturated time-dependent problems (Geo-Slope 2007).

Modeling procedure

Model parameters

Model extents are different for cross-sections A and EF, while grid type and grid size are the same for both cross-sections. Model domain for cross-section A extending in North–South direction is 1577 m in length with a unit width; however, the thickness varies between 550 and 307 m due to current mine topography. Cross-section EF extending in East–West direction is 2910 m in length, while the thickness changes between 607 and 61 m due to topography. Discretization (or gridding) is an important step in numerical modeling. Discretization is splitting the model domain into small
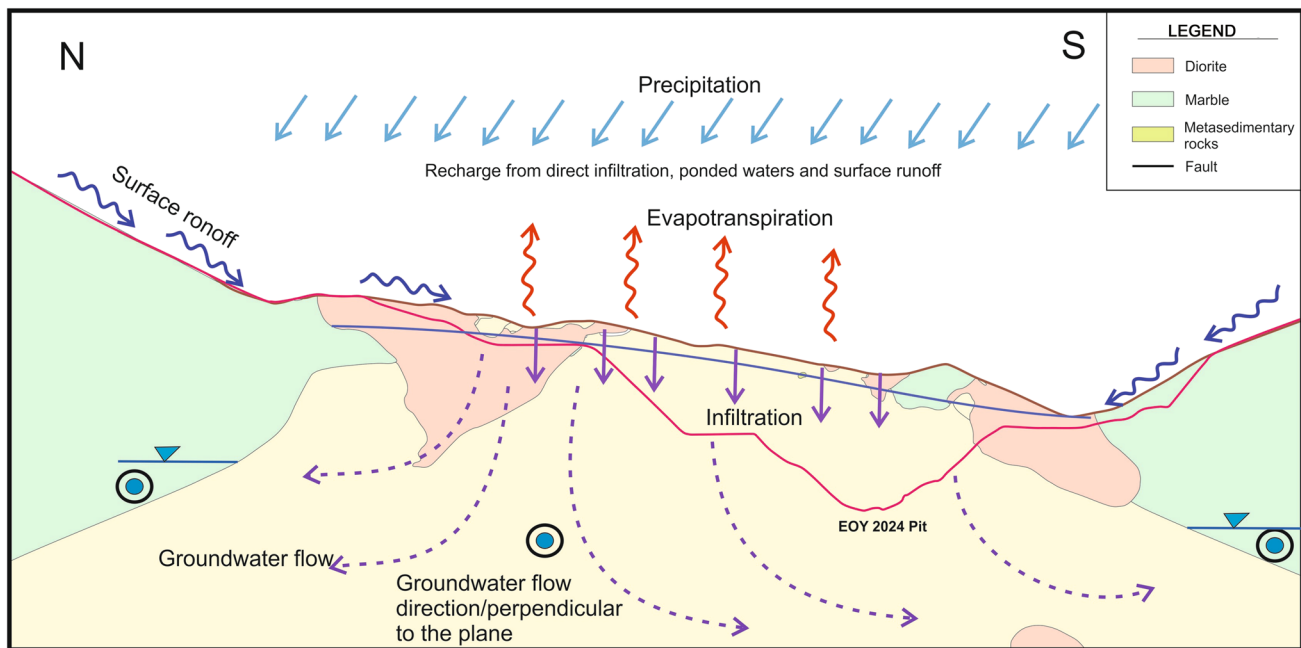
Fig. 4 Hydrogeological conceptual model of the mine site (Ekmekci et al. 2018)

blocks which are called elements. In both cross-sections, quads and triangular types of elements which range from 10 to 1 m in size are assigned to the model. Grid size around vibrating wire piezometer locations whose measured head and pore-water pressure values are used as calibration targets are assigned as 1 m to increase the accuracy. There are totally 8398 nodes and 8725 elements for cross-section A and 16,505 nodes and 16,958 elements for cross-section EF.

Cross-section A has been divided into distinct layers based on hydraulic conductivity values obtained from the packer tests, RQD, and textural properties. The results of packer tests show that coefficient of variation of hydraulic conductivities in the same hydrostratigraphic layer is quite high. This suggests that the hydrostratigraphic layers are not homogeneous in their hydraulic conductivity values both in vertical and lateral direction. Hence, metasediment–diorite block which constitutes the main flow domain is divided into distinct layers (Fig. 5). However, for cross-section EF, diorite blocks show almost uniform hydraulic conductivity values within itself. Hence, only the metasediment block has been divided into different segments based on the packer test results (Fig. 6).

At the beginning of the calibration, uniform hydraulic conductivity values are assigned for each hydrostratigraphic layer at both cross-sections and the layers are subsequently segmented into lateral zones during the calibration steps (Figs. 5 and 6). Initially, hydraulic conductivity values of the waste rock material and marble are assigned as 4.0×10^{-4} m/s and 7.0×10^{-6} m/s, respectively, based on the previous studies conducted at the site by Golder Associates

(2013). However, the pumping test conducted at well Dwb-2 located in the south part of the study area yielded a hydraulic conductivity value for Marble as 2.4×10^{-8} m/s. Hence, the hydraulic conductivity for marble at the south part of the section is updated with the current hydraulic conductivity value for marble.

At saturated flow condition, conductivity is at maximum, while, at unsaturated flow condition, hydraulic conductivity starts decreasing in relation to water content. To represent the drained behavior of materials, Soil Water Characteristic Curves (SWCC), which are converted to pressure–hydraulic conductivity relationships, are defined for each material. SWCC defines how much water will be held in the system depending on matric suction. The volumetric water content curve can be determined by grain size analysis, and laboratory and in situ analysis. Additionally, in the absence of data, the volumetric water content curve can be estimated from the literature or GeoStudio™ (Geo-Slope 2007) library. To keep the consistency between the cross-sections, same SWCC are used at both cross-sections.

SEEP/W (Geo-Slope 2007) uses the Van Genuchten estimation method, which uses saturated and residual water contents and curve-fitting parameters to draw SWC curves (Van Genuchten 1980). Saturated and residual water contents are determined from the laboratory tests performed by Ekmekci et al. 2018. These properties measured with centrifuge equivalent moisture content method due to ASTM (D425-17) standards. Metasediment–diorite block materials are defined as altered and massive based on geotechnical logs prepared by Golder Associates. Porosity and residual
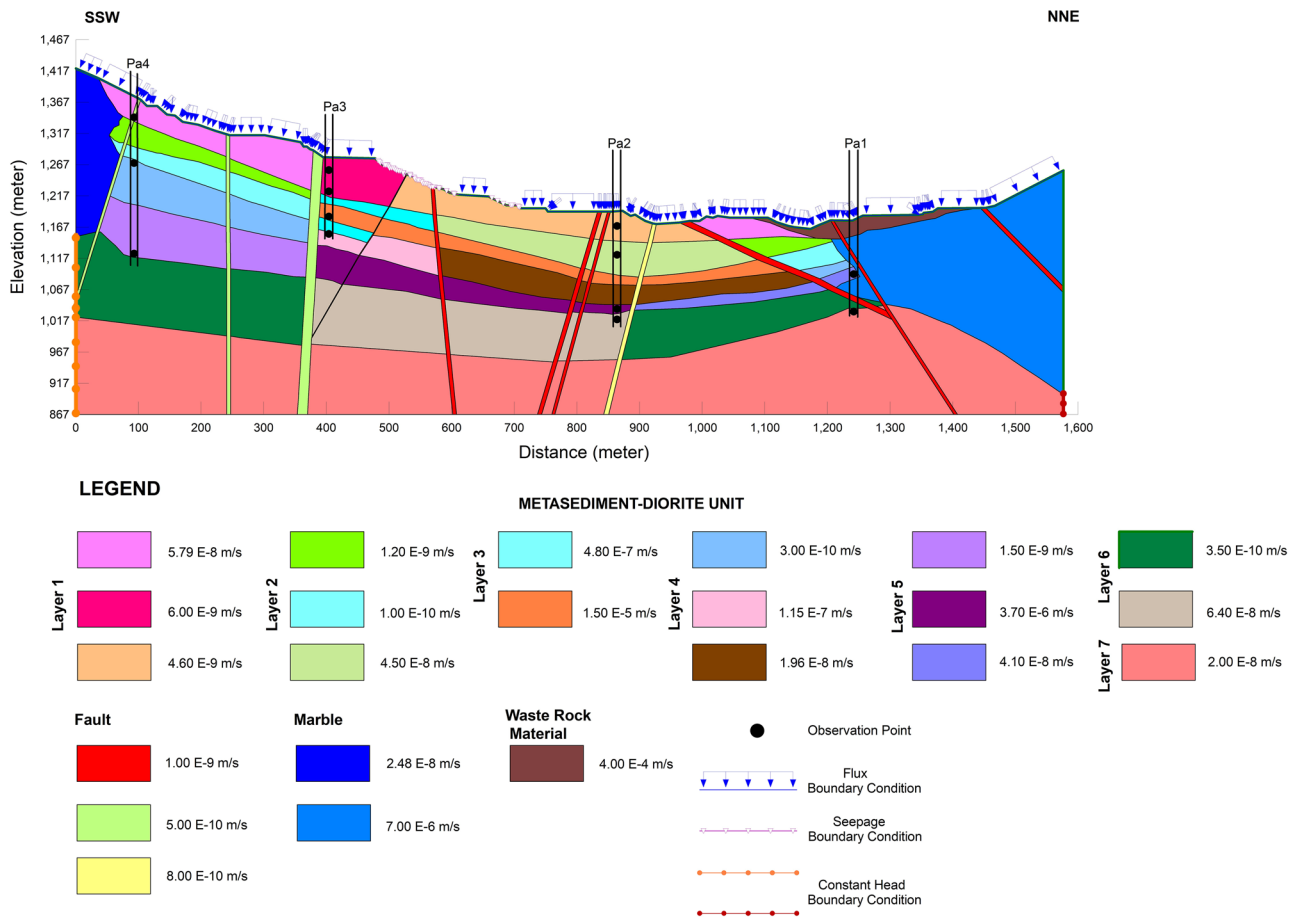
Fig. 5 Hydrostratigraphic layers with lateral zonation and calibrated hydraulic conductivity values at cross-section A
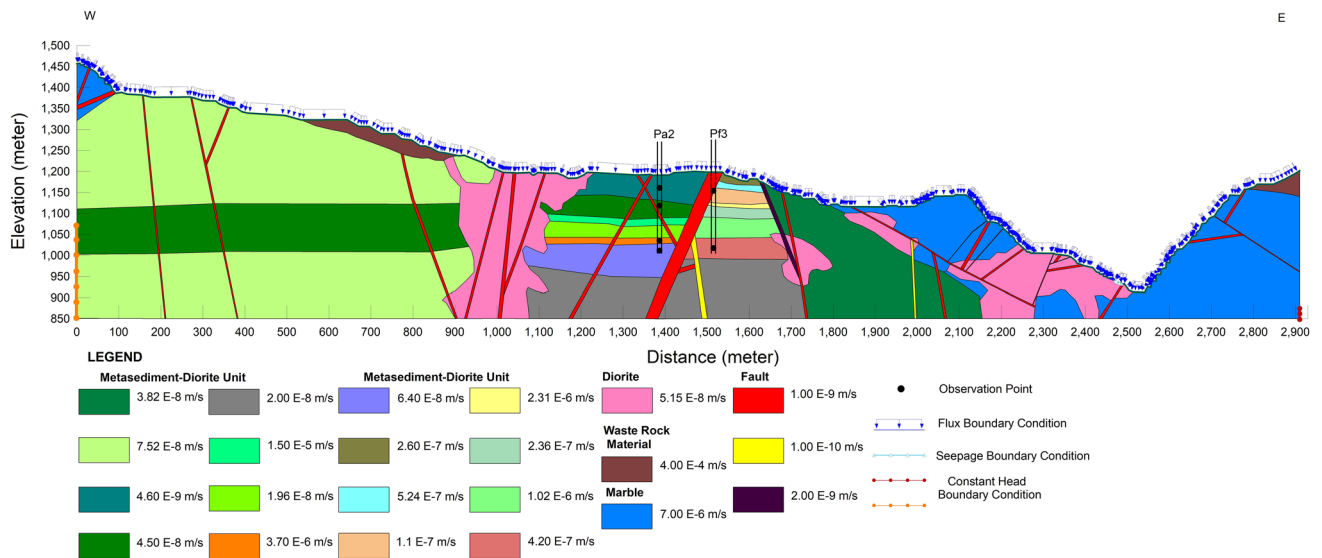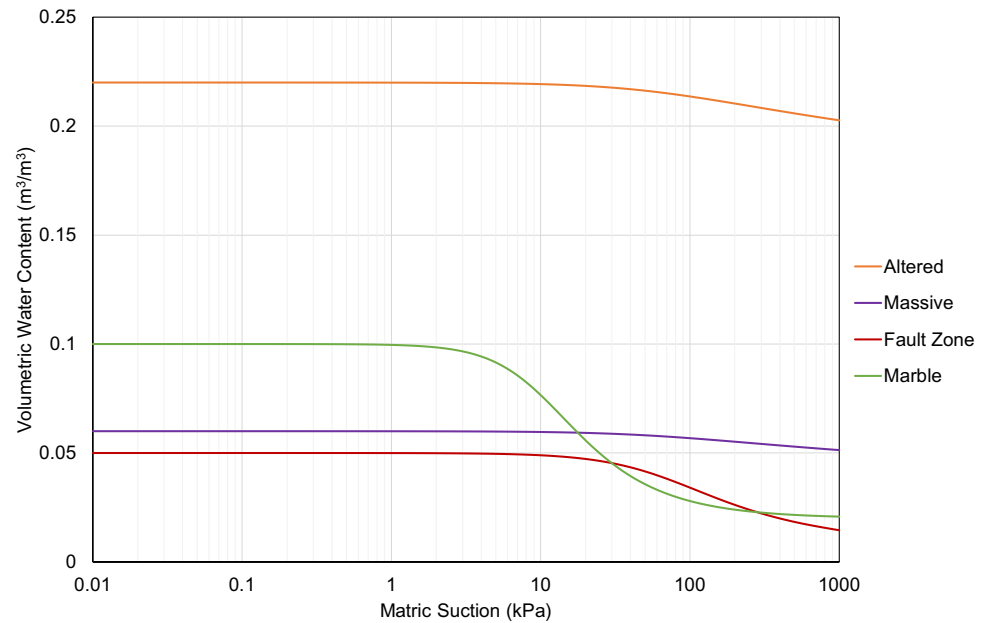

Fig. 6 Hydrostratigraphic layers with lateral zonation and calibrated hydraulic conductivity values at cross-section EF

Fig. 7 Soil water characteristic curves

water content for altered material are assigned as 0.22 and 0.18, respectively, and 0.06 and 0.04 for massive material, respectively, based on the laboratory results. Saturated water content for marble is assigned as 0.1 which is a typical porosity value for fractured rocks according to Freeze and Cherry (1979). The curve-fitting parameters in this study were obtained from the similar studies in the literature (Al-Yahyai et al. 2006; Parent and Cabral 2006; Benson et al. 2007; Argunhan-Atalay and Yazicigil 2018). The resulted SWCC curves can be seen in Fig. 7.

The faults considered throughout the model domain are those determined by Terrane Geoscience Inc. (2018) except that they are assumed to extend along the whole simulated depth. This was necessary to eliminate the effects of the bottom no-flow boundary condition and rapidly changing topography, requiring a thickness more beyond 100 m, the depth limit set by Terrane Geoscience Inc. (2018) for their evaluation. There were no hydraulic conductivity data available for the faults in the model domain. Core inspections and the significant differences between piezometric levels across the faults have clearly revealed the fact that a great majority of the faults function as impermeable barriers. Initially, a hydraulic conductivity value of 1×10^{-9} m/s was uniformly applied to all faults in the model domain. The SWCC curve for the faults shown in Fig. 7 is derived based on clay gouge infilling in most of the drilled geotechnical boreholes. During the model calibration runs, the hydraulic conductivities of the southern faults, including the South Çöpler Fault Zone, are reduced by one half to 5×10^{-10} m/s to obtain a satisfactory match between observed and simulated heads.

Boundary conditions

Model boundaries are determined based on geological and hydrogeological characteristics of the study area. To represent the groundwater flow regime, constant head boundary conditions are assigned to both end of the flow domain at both cross-sections. Groundwater level is taken as 1250 m (asl) at southern part, while it is assigned as 898 m at the northern part of the cross-section based on groundwater maps produced in different years by Golder Associates (2013) and SRK (2015) for cross-section A (Fig. 5). The observed groundwater levels that remained rather stable over the long term at both end of cross-section EF are used to assign groundwater heads of 1073 m and 870 m to the western and eastern end of the flow domain, respectively (Fig. 6). Uniform unit flux at both sections is assigned as upper boundary condition to represent the recharge that is calculated from the water budget in the mine area (Ekmekci et al. 2018). Additionally, seepage boundary condition is assigned to steep slopes of higher altitudes (i.e., present-day topography) of the model to allow the groundwater flow out of the flow domain.

Steady-state calibration

Calibration of the models was conducted under steady-state conditions by trial-and-error. There are four piezometer wells located on cross-section A and a total of thirteen vibrating wire pressure transducers were installed in these piezometers, while there are two piezometer wells located along cross-section EF and six vibrating wire pressure transducers installed (Figs. 5 and 6). Observed data from
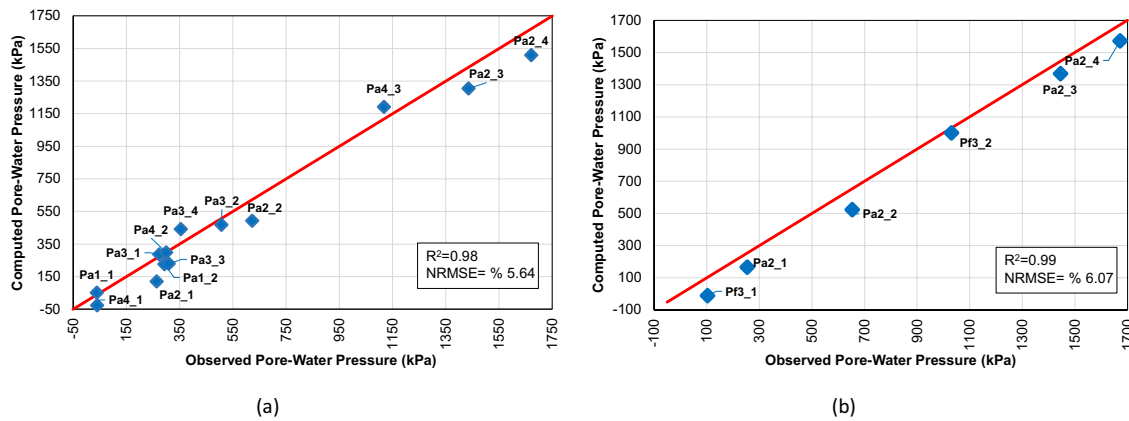
Fig. 8 Relation between simulated and measured pore-water pressure values: **a** for cross-section A, **b** for cross-section EF

these vibrating wire piezometers are used for the calibration. Goodness of fit was evaluated for total head, pore-water pressure, and pressure head values, separately. During the calibration, hydraulic conductivity values are adjusted within reasonable limits by trial-and-error until there is a good match between observed and computed values.

After several trials of calibration runs, the Root-Mean-Square Error (RMSE) for cross-section A was calculated as 6.93 m, 92.01 kPa (Fig. 8a), and 9.40 m for total head, pore-water pressure, and pressure head values, respectively. Normalized Root-Mean-Square Error (NRMSE) was calculated as 2.40%, 5.64%, and 5.65% for total head, pore-water pressure, and pressure head values, respectively. RMSE for cross-section EF was calculated as 6.54 m, 95.16 kPa (Fig. 8b), and 9.82 m for total head, pore-water pressure, and pressure head values, respectively. NRMSE was calculated as 10.52%, 6.07%, and 6.14% for total head, pore-water pressure, and pressure head values, respectively. The error statistics show that the models are capable of simulating the total head and pore-water pressure distributions along both cross-sections reasonably well (Agartan and Yazicigil 2012) and can be used successfully for further analysis.

Transient analysis

Sections A and EF were also modeled under the transient condition for 20 years (7300 days) to confirm the steady-state values obtained by assigning seasonally varying uniform recharge. It is expected that the transient run in the long term will reach a steady-state condition which is not significantly different than the generated steady-state solution. At the end of the transient analysis, it was found that most of the piezometers reach a steady-state condition before the end of the transient simulation period and the differences between those values and the steady-state computed head values are generally negligible (i.e., less than 0.25 m). Hence, it can

be concluded that the computed steady-state values can be reliably used as the initial conditions for transient analyses.

Results and discussion

In the following sections, groundwater inflow and pore-water pressure values at the open pit slopes were calculated with and without horizontal drains for both cross-sections under transient conditions for mine development in year 2019. Furthermore, the variations in volumetric water content in the wall rock in the vicinity of the slopes are evaluated and discussed.

Open pit development modeling

Expansion and deepening of the open pit along cross-sections in the year 2019 were provided by Anagold. The expansion and deepening phases of the pit through the year were implemented into the numerical model. Numerical models consist of six phases and each of them represents the two-month operational period for pit deepening. Pit bottom elevation in these models changes from 1191 to 1090 m.

Both cross-sections were modeled under the transient condition for 365 days. Initial condition of the model for phase one was taken from the calibrated models for the current topography at both cross-sections. In the following steps, the initial condition of each phase was taken from former phase results. Material properties are exactly the same as the previous models (see Figs. 5 and 6). All boundary conditions were kept the same with calibrated models except the recharge boundary conditions. Boundary condition of the upper surface of the open pit was modified from flux boundary condition that represents recharge into the mine to seepage face boundary condition. The in-pit recharge is

assumed to be controlled and diverted away from the pit by the surface water channels.

At both cross-sections, the hydraulic gradients were not reversed until the pit bottom elevation reaches to 1184 m. Thereafter, reversals in hydraulic gradients start to take place with successively increasing gradients and groundwater inflow rates as the pit bottom is deepened. The results, however, show that layering of hydraulic conductivity produced by various hydrostratigraphic layers encountered as pit bottom is deepened produce variations in the amount of groundwater inflow toward the pit. At cross-section A,

groundwater inflow toward the pit mainly takes place from south slope and pit bottom, and groundwater inflow from the northern part is quite minor (Table 1). At cross-section EF, groundwater inflow to the pit is mainly from the west slope and pit bottom. However, as the pit bottom elevation decreases, there is also groundwater inflow from east direction (Table 1). This is mainly due to the presence of lower constant head boundary conditions in the north and east end of the sections. When both sections are considered together, it can be summarized that there is groundwater inflow from

Table 1 Groundwater inflow amounts into open pit at different phases

| Phase no. | Pit bottom elevation (m) | Without horizontal drain condition | | | | | | With horizontal drain condition | | | |
| | | Cross-section A (L/day/m) | | | Cross-section EF (L/day/m) | | | Cross-section A | | Cross-section EF | |
		South	Bottom	North	West	Bottom	East	South (L/day/m)	Change in inflow rates (%)	West + east (L/day/m)	Change in inflow rates (%)
1	1184	0.00	11.53	0.00	0.00	0.00	0.00	0.00	0.00	0.00	0.00
2	1173	54.92	47.70	0.00	11.64	20.16	0.00	60.66	10.45	11.64	0.00
3	1158	103.93	200.00	0.95	25.57	90.82	0.00	136.07	30.91	25.57	0.00
4	1140	141.29	513.39	0.00	58.87	368.06	4.84	193.55	36.99	72.58	13.92
5	1120	120.00	444.92	2.95	189.34	634.26	70.66	163.93	36.61	300.49	15.57
6	1090	418.52	159.18	70.82	304.10	572.13	307.38	576.56	37.76	708.75	15.91
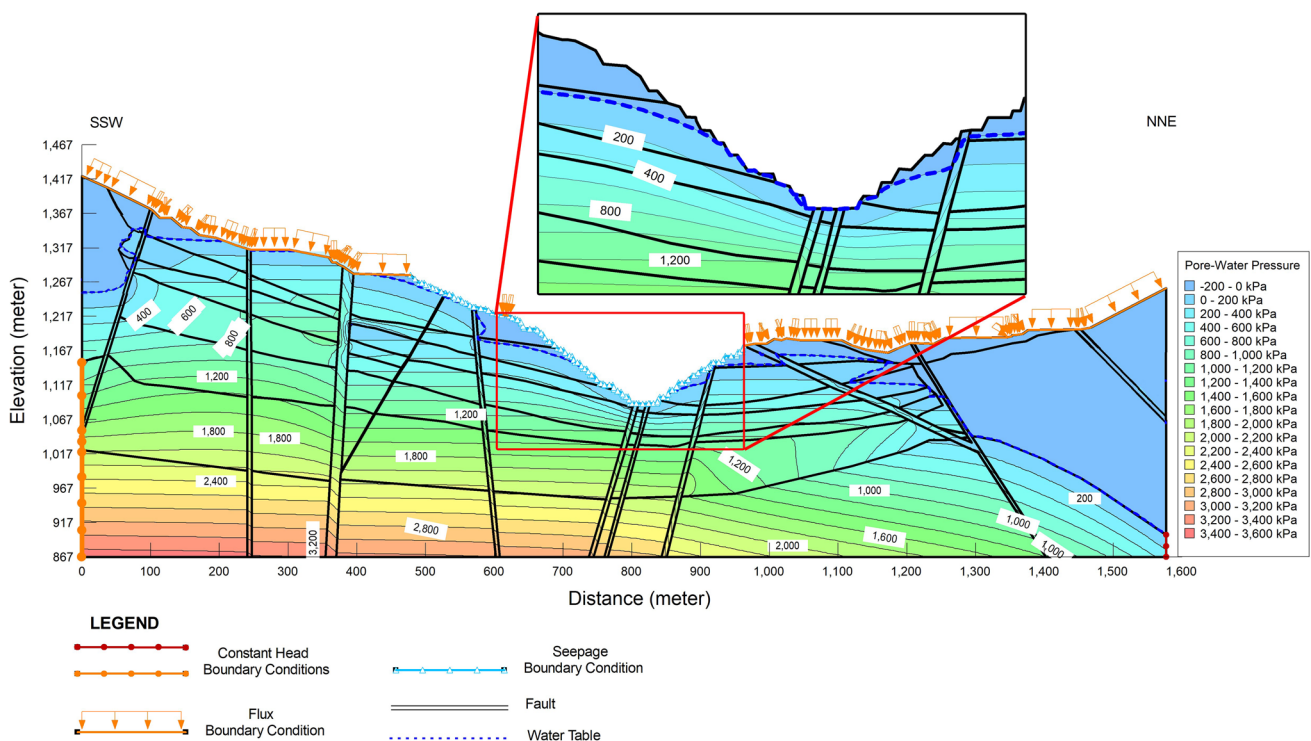
Fig. 9 Pore water pressure when the pit bottom elevation is lowered by 100 m at cross-section A (end of Phase 6)
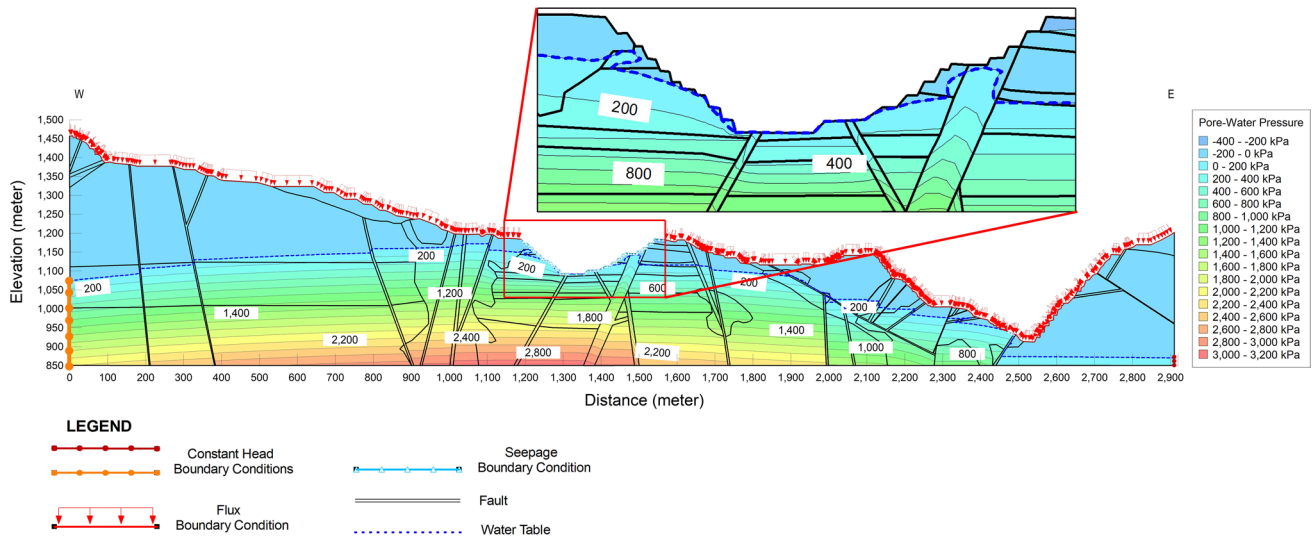
Fig. 10 Pore water pressure when the pit bottom elevation is lowered by 100 m at cross-section EF (end of Phase 6)

south, west, and east slopes toward the pit, the greatest flux being through the bottom of the pit.

Additionally, south, west, and east slopes are under saturated conditions at the end of the simulation for year 2019 (Figs. 9 and 10). This may require the implementation of a slope depressurization program. To drain the groundwater

inflow and dissipate the high pore-water pressure behind the pit walls, horizontal drains were implemented into numerical models at both cross-sections.
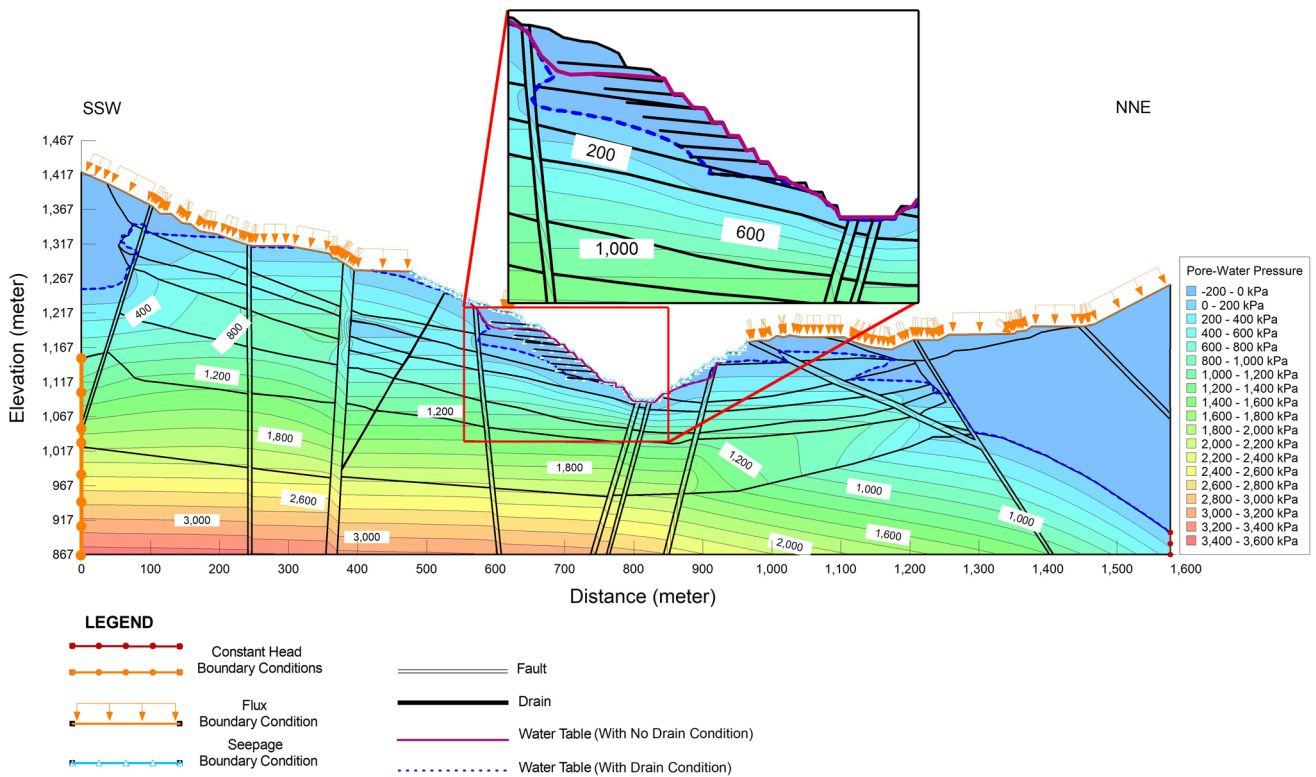
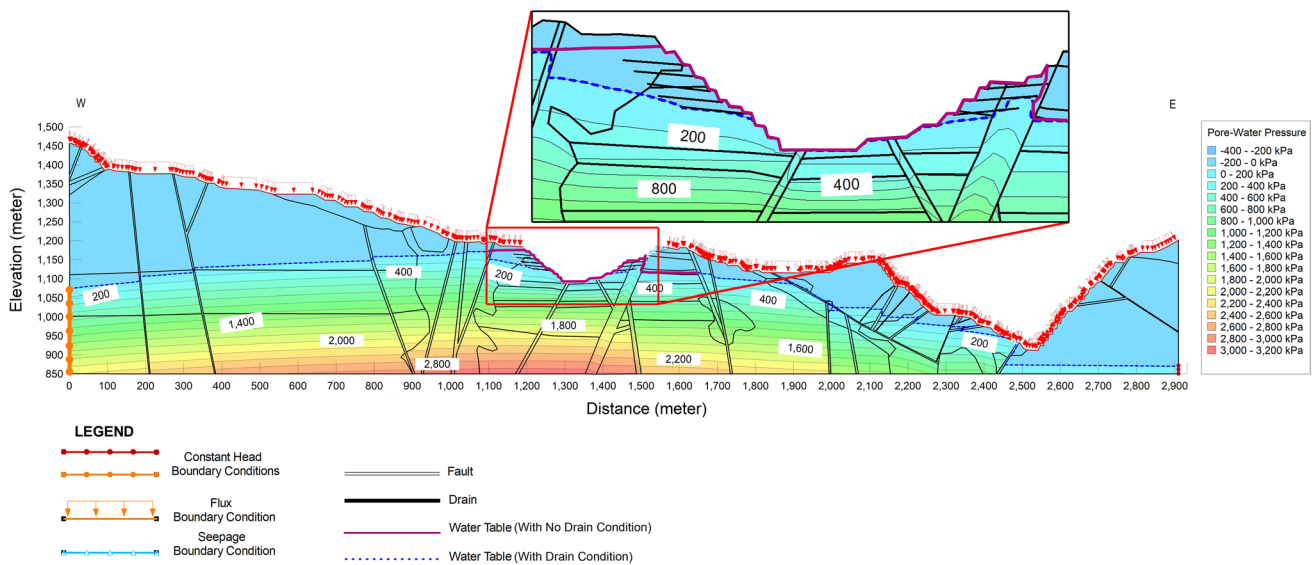**Fig. 11** Pore water pressure distribution after the use of horizontal drains at cross-section A

Fig. 12 Pore water pressure distribution after the use of horizontal drains at cross-section EF

Simulation with horizontal drains

For the purpose of depressurization, horizontal drains which are 50 m in length with a 5° inclination were installed at different elevations (Figs. 11 and 12). The vertical distance between horizontal drains varies between 10 and 14 m based on the pit advancement. Each horizontal drain was specified as a line with a seepage face boundary condition (Rahardjo et al. 2003). At cross-section A, nine rows of horizontal drains were installed on the south slope. In cross-section EF, 5 rows of horizontal drains were installed on the west slope, while 3 rows on the east slope. Flux lines were used in the model around each drain location and on the slope surface to calculate the groundwater inflow amount. As can be seen in Table 1, groundwater inflow reaches its maximum value from south, west, and east slopes at phase 6 in both cross-sections. To evaluate the effectiveness of horizontal drains, calculated inflows and change in flux amount in each phase at the models (the one with horizontal drains and the one with no drains) are given in Table 1. The installation of horizontal drains although seems to be effective in lowering the groundwater table, and they are ineffective in reducing the volumetric water content and improving the amount of groundwater drained significantly. With the presence of horizontal drains, groundwater inflow rates drained were increased by 15 and 37% for sections EF and A, respectively, as compared to the models with no horizontal drains. Although there are no horizontal drains installed with the same characteristics (ideal construction and fully draining) and locations as modeled herein to validate these results, the groundwater inflow rates drained by some horizontal drains installed earlier at the site support the results

obtained. As part of the slope depressurization program, 35 horizontal drains (varying between 50 and 75 m in length) were installed along benches with different elevations in 2016. The total amount of groundwater drained from six horizontal drains close to the Section A installed along the bench at 1250 m was less than 0.1 L/min. The numerical model results show that the amount of groundwater drained at level 1120 m is around 0.23 L/min. The amount of simulated drained water is higher compared to the measured one, because simulated horizontal drains are at lower elevation than the measured ones. Furthermore, the simulated drains are assumed to be ideally constructed with fully draining characteristics, conditions that are not always met under field conditions. From this perspective, it can be stated that the field measurements support the results of the numerical models whereby it was demonstrated that the efficiency of dewatering the slopes is not significantly increased by the horizontal drains.

The models with horizontal drains show lowering of the groundwater table in the vicinity of the slopes (Figs. 11 and 12). The close-up views, showing the immediate vicinity of the pit at both cross-sections, are depicted in Fig. 13. The dissipation of pore-water pressures at two points located on vertical and inclined sections that are parallel to the slope face at south, west, and east slopes are given in Fig. 14a through c, respectively. The examination of these figures show significant reduction (175–350 kPa) in pore-water pressures at all slopes except the east slope where the selected point is within a fault zone. However, the saturation conditions at the wall rocks are more important than lowering of the groundwater table or pore-water pressures for the slope stability. To evaluate the saturation conditions, the
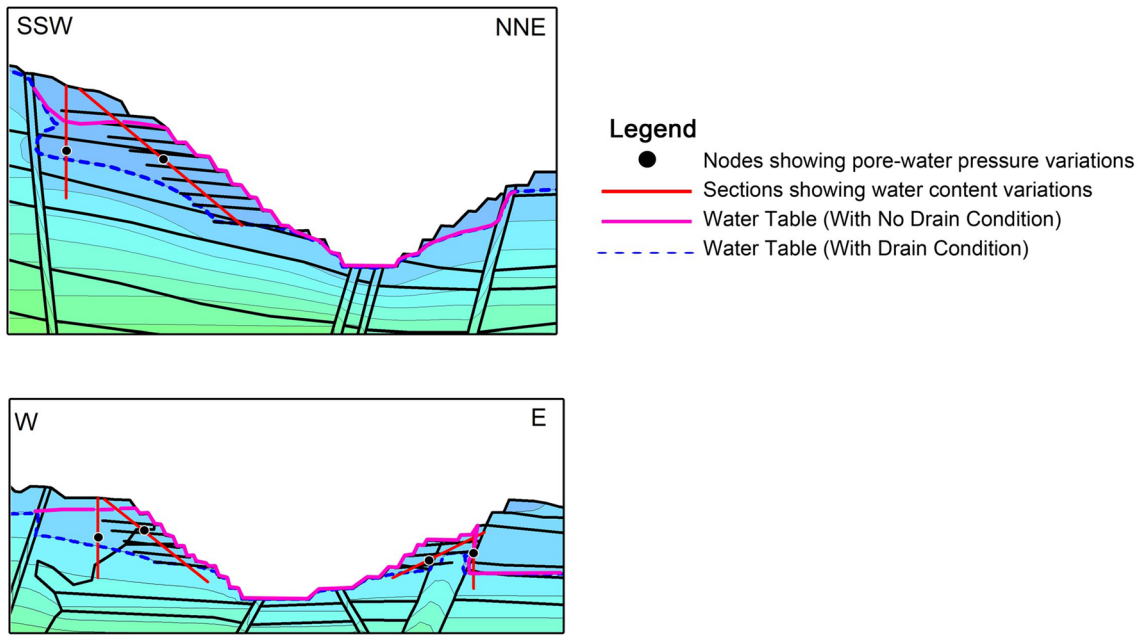
Fig. 13 The close-up views in the vicinity of pit at both cross-sections
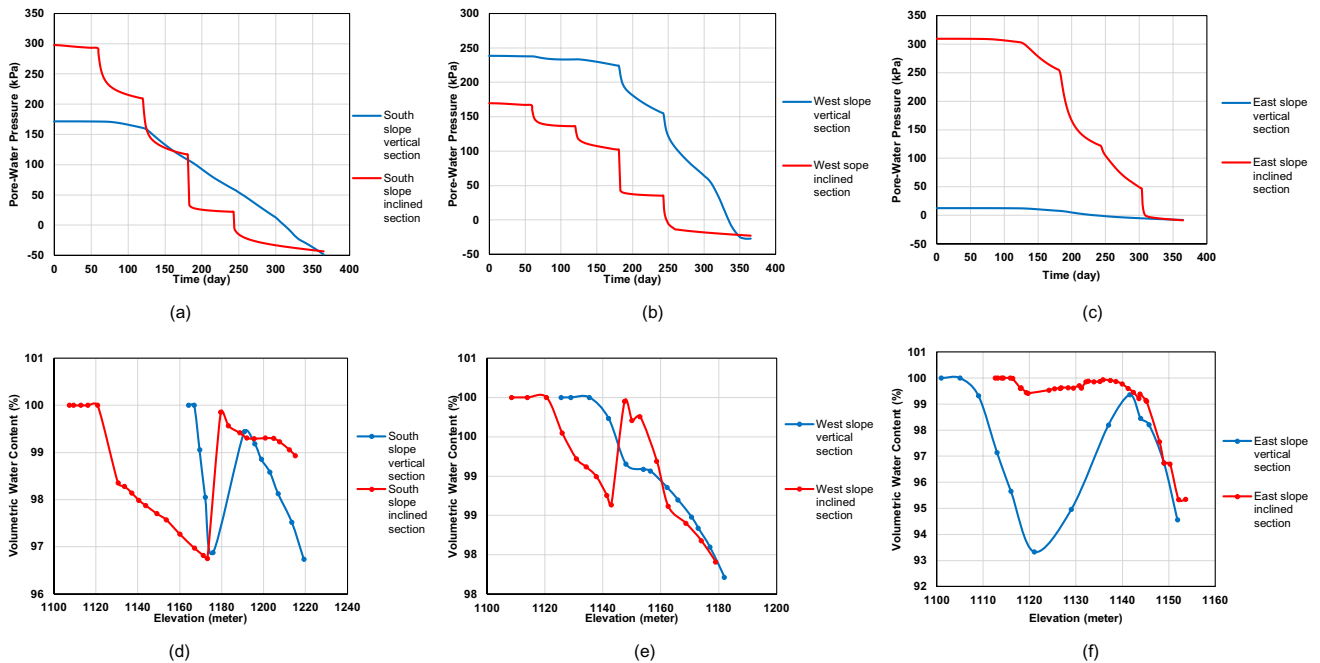

Fig. 14 Change of pore-water pressure and volumetric water content percentage at all slopes after the use of horizontal drains

volumetric water content percentages at south, west, and east slopes are analyzed along vertical and inclined sections that are parallel to the slope face, as shown in Fig. 14d through f. Although significant reductions in pore-water pressures are achieved with the use of horizontal drains, the amount of water content along selected sections at all slopes is almost close to fully saturation state (93–100%) (Fig. 14). Hence, the saturation state in the wall rock in the vicinity of the slopes is more critical for achieving slope stability. Thus, based on both the volumetric water content percentage and the amount of drained water, it can be concluded that the use of horizontal drains is not effective in the study area.

Conclusion

This paper aimed to evaluate the effectiveness of horizontal drain holes in achieving dissipation of pore-water pressures in the wall rock within the desired time period required for mining at Çöpler Mine site. This aim required the work carried out to understand the hydrogeological conditions within the Çöpler Mine site, and to develop conceptual and numerical models to predict the pore-water pressure distribution along selected cross-sections. Mining operations take place mainly in metasediment and diorite units. Although they exhibit similar properties, faulting, folding, and different degree of alteration increase the heterogeneity within these units. The heterogeneity was described using packer test, texture, and RQD results. Prior to development of numerical model, conceptual model was developed by the help of geological and hydrogeological data. 2D numerical model SEEP/W was used to determine the pore-water pressure distribution in two critical cross-sections which are in North–South and East–West direction. The model was calibrated for steady-state conditions by trial-and-error for each cross-section using the data of pore-water pressures measured in the piezometers by vertically distributed vibrating wire piezometers. Goodness of fit between the observed and simulated values was analyzed for total head, pore-water pressure, and pressure head values, separately. The calibrations were considered to be acceptable when the normalized error is below 10%. The transient run in the long-term reached a steady-state condition which is not significantly different than the generated steady-state solution, suggesting that the computed steady-state values can be reliably used as the initial conditions for further analysis. The expansion and deepening phases of the pit through the year 2019 were implemented into numerical models. The groundwater flux into the pit mainly comes from south, west, and east slopes and the bottom of the pit. The results further demonstrate that backward of these three slopes remains under saturated condition which may require the implementation of a slope depressurization program.

To drain out groundwater and relieve the pore-water pressure in saturated slopes, horizontal drains were simulated in the numerical models and the results were analyzed. The installation of horizontal drains although seems to be effective in lowering the groundwater table and reducing the pore-water pressures, they are ineffective in reducing the volumetric water content and improving the amount of groundwater drained significantly. Although significant reductions in pore-water pressures are achieved with the help of horizontal drains, the amount of water content is almost close to fully saturation state. Thus, it can be concluded that the use of horizontal drains to achieve slope stability is not effective in the study area; a finding previously confirmed by

the company who installed horizontal drains. A management strategy consisting of elimination of the ponding and infiltration of surface runoff by constructing diversion ditches lined with impervious liners was demonstrated to be more effective and practical approach to managing groundwater impacts on slope stability at the mine.

In addition to its contribution to control of slope stability, this study illustrates the importance of data gathering, in spite of the initial cost which may be a small percentage of the potential benefits obtained. In complex hydrogeological settings, a program consisting of in situ data collection, characterization, conceptual and numerical model development, and monitoring reduces the degree of uncertainty related to distribution of pore-water pressures and saturation conditions. The results presented are expected to be of value to the database of experience of the mining industry in understanding how various rock types with particular characteristics react under various drainage/depressurization scenarios.

References

Agartan E, Yazicigil H (2012) Assessment of water supply impacts for a mine site in western Turkey. Mine Water Environ 31:112–128

Alacer Gold (2016) Çöpler mine NI 43-101 technical report. Çöpler, Erzincan (**Unpublished**)

Al-Yahyai R, Schaffer B, Davies FS, Munoz-Carpena R (2006) Characterization of soil-water retention of a very gravelly loam soil varied with determination method. Soil Sci J 171:85–93

Argunhan-Atalay C, Yazicigil H (2018) Modeling and performance assessment of alternative cover systems on a waste rock storage area. Mine Water Environ 37:106–118

Beale G, Read J (2013) Guidelines for evaluating water in pit slope stability. Csiro, Canberra

Benson CH, Sawangsuriya A, Trzebiatowski B, Albright WH (2007) Postconstruction changes in the hydraulic properties of water balance cover soils. J Geotech Geoenviron Eng 133(4):349–359

Brehaut RJ (2009) Groundwater, pore pressure and wall slope stability—a model for quantifying pore pressures in current and future mines. PhD Dissertation, University of Canterbury, New Zealand

Cano M, Tomás R (2013) Assessment of corrective measures for alleviating slope instabilities in carbonatic Flysch formations: Alicante (SE of Spain) case study. Bull Eng Geol Environ 72:509–522

Douglas B, Mercer S, Wright S, Barclay D (2009) Pit water management in a mine planning cycle, olympic dam case study. Min Technol 118(3–4):115–130

Ekmekci M (2012) Usage possibilities of the water pressure test in characterization of rock aquifer. In: 65th years Mahir Vardar-geomechanics, tunneling and design of rock structures—special sessions, Istanbul, pp 521–535

Ekmekci M, Yazicigil H, Argunhan-Atalay C, Tayyar D, Kalkan F (2018) Optimization of groundwater control for slope stability at Çöpler Mine Site. Anagold Madencilik San. ve Tic. A.Ş., Hacettepe Mineral Technologies (HMT), Ankara (**Unpublished**)

Freeze RA, Cherry JA (1979) Groundwater. Prentice-Hall Inc, New Jersey

Geo-Slope (2007) Seepage modeling with SEEP/W 2007 an engineering methodology. Geo-Slope International Ltd, Calgary

Ghiassian H, Ghareh S (2008) Stability of sandy slopes under seepage conditions. Landslides 5:397–406

Golder Associates (2013) Integrated surface water and groundwater studies of Copler mine sulfide expansion project. Anagold Madencilik San. ve Tic A.Ş., Ankara

Harman J, Hormazabal E, Martinez S (2007) Fact and fiction about pit slope depressurisation. In: Potvin Y (ed) Slope stability. ACG, Perth

Jia GW, Zhan LT, Chen YM, Fredlund DG (2009) Performance of a large-scale slope model subjected to rising and lowering water levels. Eng Geol 106:92–103

Leech S, McGann M (2008) Open pit slope depressurization using horizontal drains—a case study. In: 10th International Mine Water Association Congress, Karlsbad, Czech Republic

Martin RP, Siu KL, Premchitt J (1994) Review of the performance of horizontal drains in Hong Kong. In: Special project report, SPR 11/94, Geotechnical Engineering Office, Civil Engineering Department, Hong Kong, p 106

McCabe GJ, Markstrom SL (2007) A monthly water-balance model driven by a graphical user interface. In: USGS Open-File report 2007–1088, Virginia, USA

McNicholl DP, Pump WL, Cho GWF (1986) Groundwater control in large scale slope excavations histories from Hong Kong-five case. In: Cripps JC, Bell FG, Culshaw M (eds) Groundwater in engineering geology. The Geological Society London, London, pp 513–523

Moharrami A, Hassanzadeh Y, Salmasi F, Moradi G, Moharrami G (2014) Performance of the horizontal drains in upstream shell of earth dams on the upstream slope stability during rapid drawdown conditions. Arab J Geosci 7:1957–1964

Mukhlisin M, Abd Aziz NAB (2016) Study of horizontal drain effect on slope stability. J Geol Soc India 87:483–490

Ozgul N, Tursucu A, Ozyardımcı N, Senol M, Bingol I, Uysal S (1981) Munzur dağlarının jeolojisi, report no.6995. Mineral research

and Exploration Institude of Turkey (MTA), Ankara, p 136 (**Unpublished**)

Parent SE, Cabral A (2006) Design of inclined covers with capillary barrier effect. Geotech Geol Eng 24(3):689–710

Rahardjo H, Hritzuk KJ, Leong EC, Rezaur RB (2003) Effectiveness of horizontal drains for slope stability. Eng Geol 69:295–308

Rahardjo H, Santoso VA, Leong EC, Ng YS, Hua CJ (2011) Performance of horizontal drains in residual slopes. Soils Found 51(3):437–447

Resnick GS, Znidarcic D (1990) Centrifugal modeling of drains for slope stabilization. J Geotech Eng 116(11):1607–1624

Roeper T, Soukup W, O'Neill R (1992) The applicability of the lugeon method of packer test analysis to hydrogeologic investigations. Groundwater 8(3):29–36

Singh TN, Pradhan SP, Vishal V (2013) Stability of slopes in a fire-prone mine in Jharia Coalfield, India. Arab J Geosci 6:419–427

Solak KC, Tuncay E, Ulusay R (2017) An investigation on the mechanisms of instabilities and safe design of the south slope at a lignite pit (SW Turkey) based on a sensitivity approach. Bull Eng Geol Environ 76:1321–1341

SRK (2015) Volume 1: ESIA report on the çöpler gold mine sulfide expansion project, appendices, report/project number: 941003. Anagold Madencilik San. ve Tic A.Ş., Ankara

Terrane Geoscience Inc (2018) Report on structural mapping and 3d fault modeling, Çöpler Mine, Central Turkey. Anagold Madencilik San. ve Tic A.Ş., Ankara

Ulusay R, Ekmekci M, Tuncay E, Hasancebi N (2014) Improvement of slope stability based on integrated geotechnical evaluations and hydrogeological conceptualization at a lignite open pit. Eng Geol 181:261–280

Van Genuchten MT (1980) A closed form equation for predicting the hydraulic conductivity of unsaturated soils. Soil Sci Soc Am J 44:892–898

Vaskau P, de Quadros EF, Kanji MA, Johnson T, Ekmekci M (2019) ISRM suggested method for the lugeon test. Rock Mech Rock Eng 52:4155–4174

Williams J, Rathbone S, Campbell L (2007) Depressurization of open pit walls-a practical example from the South East Prongs Pit, Tom Price, Western Australia. In: Potvin Y (ed) Slope stability . ACG, Perth